Al-Azhar University Civil Engineering Research Magazine (CERM)
Vol. (39) No. (2) April, 2017

HYSTERETIC BEHAVIOR OF STEEL FIBER REINFORCED CONCRETE BRIDGE COLUMNS REPAIRED WITH EXTERNALLY BONDED CFRP

Abdel-rahman Mohamed Naguib [a], Nayer Ahmed El-Esnawy [b], Ahmed Mahmoud Saleh [c], Waleed Abdel-latif Atteya [c]

[a] Lecturer Assistant, Civil Engineering Department, MTI University, Cairo, Egypt, and PhD candidate, Dept. of Structural Engineering, Cairo University, Giza, Egypt

[b] Professor, Dept. of Structural Engineering, Cairo University, Giza, Egypt (on leave as Head of Civil Engineering Department, Faculty of Engineering and Technology, Badr University in Cairo, Egypt)

[c] Professor, Dept. of Structural Engineering, Cairo University, Giza, Egypt

ملخص: يؤدى إضافة الألياف الحديدية إلى الخرسانة المسلحة إلى إكسابها العديد من الخصائص المفيدة. من بين هذه الخصائص هو الحفاظ على وحدة وتماسك العناصر بالإضافة الى زيادة المرونة. و تعتبر هذه الخصائص هامة فى حالة ترميم العناصر من الأضرار الناتجة عن التأثير الزلزالى. بعض المواصفات العالمية تذكر مفهوم "الترميم العاجل للكبارى لإستعادة الخدمات العاجلة بعد حدوث التأثير الزلزالى" . فى هذه المواصفات يتقيد المدى الزمنى لعملية الترميم بثلاثة أيام ، و بالتالى يتم إستبعاد كافة مواد الترميم ذات الأساس الأسمنتى. تعتبر المواد ذات الأساس الإيبوكسي بالإضافة إلى ألياف الكربون بديل جيد. بالإضافة إلى ذلك يتميز هذا البديل بالحفاظ على الأبعاد الأصلية للعناصر و بالتالى الحفاظ على الجساءة النسبية بين العناصر الإنشائية المختلفة للمنشأ بدون تعديل بعد عملية الترميم. تم دراسة السلوك الزازالى لأربعة نماذج مصغرة بنسبة ١:٤ لأعمدة الكبارى تحت تأثير حمل جانبي ترددى بمعدل بطيء في وجود قوة محورية ضاغطة علي العمود بقيمة ثابتة. هذه العينات كان قد لحقها أضرار نتيجة إختبار سابق مماثل ثم تم ترميمها بإستخدام ألياف الكربون. تم دراسة تأثير المتغيرات التالية: محتوى الألياف الحديدية و نسبة الحديد الطولى و العرضى. وتم توحيد أعمال الترميم لكافة العينات. ثم تم عمل مقارنة تفصيلية للسلوك الزلزالى بين العينات التى تم ترميمها و العينات الأصلية. و قد أظهرت النتائج مدى الأستفادة من إستخدام الخرسانة المسلحة بالألياف الحديدية فى أعمدة الكبارى من حيث تسهيل و تقليل تكلفة أعمال الترميم.

Abstract: Using Steel fibers in reinforced concrete provides the structure with useful properties. Among these properties, retaining structural integrity and increasing concrete ductility. These properties are very helpful in the repairing process of seismically damaged structure elements. Some international standards introduce the concept “Rapid repair of bridges for emergency service restoration after earthquake actions”. In which, repair duration should be bounded by three days; therefore all cement based materials are excluded. Epoxy based materials combined with carbon fiber laminates are considered good alternative. In addition, this option has the advantage of retaining the dimension of original elements and therefore keeping relative stiffness between structural elements of the structure approximately unchanged after repair. The hysteretic behavior of four repaired quarter-scaled bridge columns was examined via quasi-static tests of repeated lateral loading and unloading of the scaled bridge columns when subjected to a dead axial compressive force. These specimens were experienced from damage during previous same test, and were repaired with CFRP. The parameters considered are the steel fiber content, as well as the longitudinal and lateral reinforcement ratios. The repair works were kept the same for all specimens. Detailed comparison between the hysteretic behavior of the repaired and original

specimens were developed. Results showed the benefit of using steel fiber reinforced concrete in bridge columns in terms of facilitate and reduce the cost of the repair works.

Keywords: Steel fibers; SFRC; Hysteretic behavior; Bridge columns; Ductility; Earthquake response; Quasi-static tests; Repair; CFRP.

1. INTRODUCTION

Concrete integrity can be retained by adding random discrete links represented by the steel fibers to the ingredients of concrete during the mixing process [1]. The concept of crack bridging through discrete steel fibers is introduced in ACI 544.1R-96, ACI 544.2R-89, ACI 544.3R-93, ACI 544.4R-88, ACI 544.5R-10 [2-6], and EN 14889-1:2006 [7]. The properties of steel fibers and the manufacturing details are listed in ASTM A820 / A820M – 11[8]. This criterion is important for rehabilitation of structures after earthquake excitation. The repair procedure is chosen based on the damage state of the structure and the time frame allowed for the repair process. ATC-18 [9] introduces the concept "Rapid repair of bridges for emergency service restoration after earthquake actions". In which, repair duration should be bounded by three days. This requires integer elements to save repair effort and time.

As the rehabilitation procedures vary from case to another, many Egyptian researchers tried to investigate the different strengthening and repair techniques for reinforced concrete. Strengthening and repair may be achieved by using Concrete jackets [10], Steel jackets [10], Glass fiber reinforced polymers (GFRP) wrapping [10-13], Carbon fiber reinforced polymer (CFRP) strips [11,14], CFRP wrapping [11,12]. Advantages and limitations of each repair technique were reported in terms of mode of failure, stiffness, strength, ductility, dissipated energy, cost, time consuming, and durability.

Abroad, He et al. [15] investigated the repair of five large scale reinforced concrete square columns experienced from damage due to different loading combinations of bending, shear, and torsion in previous tests. The rapid repair concept stated in the ATC-18 was obeyed. Quickset repair mortar as well as externally bonded longitudinal and transverse CFRP sheets were used in the repair process. Results showed the ability of the proposed repair process to restore the stiffness and ductility capacity of the columns to levels that can meet the needs of a temporary repair and allow emergency use after an earthquake.

There is a lack of information about the repair of steel fiber reinforced concrete (SFRC). In this study, the issue of using externally bonded CFRP as repair material for SFRC is explored. Also, the benefit of using SFRC in bridge columns for resisting earthquakes is investigated on the basis of repair. The hysteretic behavior of four repaired quarter-scaled bridge columns was examined via quasi-static tests of repeated lateral loading and unloading of the scaled bridge columns when subjected to a dead axial compressive force. These specimens were experienced from damage during previous same test. According to ATC-18 time frame, all cement based materials are excluded. Many different codes [16,17] support the use of epoxy based materials combined with carbon fiber laminates as good alternative. In addition, this option has the advantage of retaining the dimension of original elements and therefore keeping relative stiffness between structural elements approximately unchanged. The parameters considered are the steel fiber content, as well as the longitudinal and lateral reinforcement ratios. The

repair works were kept the same for all specimens. Detailed comparison between the hysteretic behavior of the repaired and original specimens were developed.

2. EXPERIMENTAL PROGRAM

The experimental program investigates the hysteretic behavior of reinforced concrete bridge columns repaired with CFRP. Four quarter-scaled bridge columns (300x400x2100 mm) with shear span of 1800 mm have been tested. The dimensions were selected such that shear span to depth ratio is 6.0, which ensures flexure dominated failure mode. A dead axial compression force of 15% the nominal load (equal to 588 KN) has been applied to all scaled columns via a hydraulic jack. All specimens had longitudinal steel bars ratio of 2.54% except S7. The control column with no steel fiber content is denoted by S1. In the meantime, S2 includes steel fiber dosages of 0.75% by volume. In column specimen S6, steel fiber dosage is 1% is used and no doubling of stirrups at plastic hinge zone exists. In column specimen S7, steel fiber dosage of 1% is used and the longitudinal steel bars ratio is 2.12%. All specimens have lap splices at mid height. Fig. 1 shows main details of all tested scaled columns.

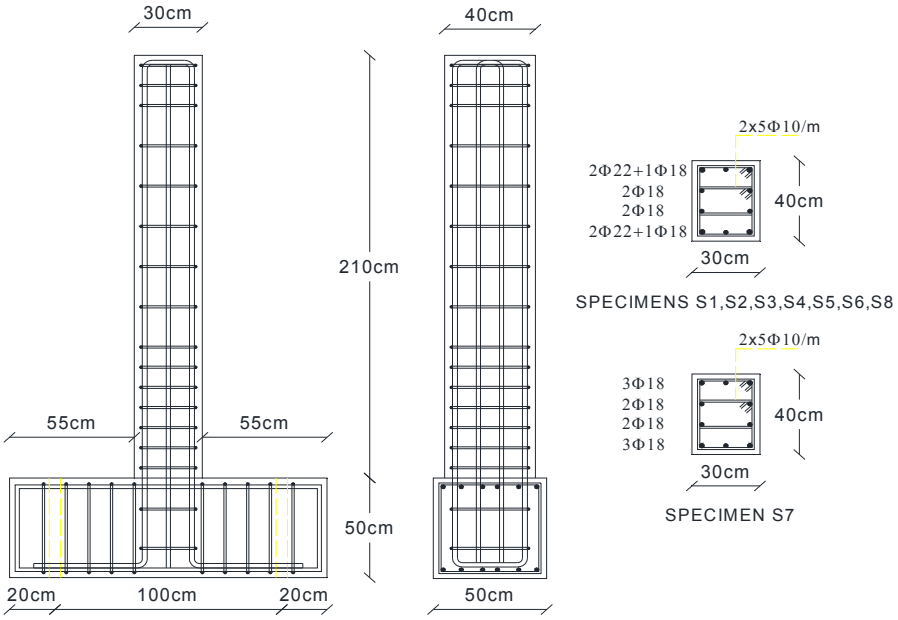

Fig. 1: Details of tested scaled bridge columns [1]

2.1 Material Properties

Details and properties of concrete ingredients, reinforcement, and steel fibers can be found elsewhere [1]. All repair materials brought from SIKA EGYPT; a leading construction materials company in Egypt [18]. Due to three days time frame for repair process, all cement based materials are excluded. Four repair materials were used in this study; Skiadur31CF, Sikadure501 Filler, Skiadur330 epoxy resin, Skiawrap230C. To compensate loose concrete, the epoxy non shrinkage mortar Skiadur31CF was chosen. It consists of two component adhesive and repair mortar based on a combination of epoxy resins and specially selected high strength fillers. Its initial setting time is 40 minutes at +20 °C, and it reaches 60-70 N/mm^2 after 24 hours at +20 °C. In order to reduce the repair cost, Skiadur31CF can be mixed with

Sikadure501 Filler; which is a kind of quartz sand with mixing ratio 1:1. To counteract the formation of transverse cracks and to provide lateral confinement of the plastic hinge zone, longitudinal and transversal layers of Skiawrap230C were glued to the plastic hinge zone. It is a unidirectional woven carbon fiber fabric for the dry application purposes. Its nominal tensile strength is 4300 N/mm^2, its nominal elongation at break is 1.8%. It should be glued to the surface using Skiadur330 epoxy resin. It is two part epoxy based impregnating resin. Its initial setting time is 60 minutes at +23 °C. Dry application means that epoxy resin should be painted first, and then the dry CFRP applied next.

2.2 Repair Procedure

The repair procedure followed the precautions stated in the Egyptian Code of Practice for the Use of Fiber Reinforced Polymer (FRP) in the Construction Fields [16]. First removing the damaged loose concrete using manual hammering, then use the compressed air to remove the dust, no water is allowed in the process. No ruptured steel reinforcement was found, therefore no need to add any extra reinforcement. Surface preparation or the sub base layer with rounded corners is used to compensate the damaged concrete. Sub base layer was made using Skiadur31CF and Sikadure501 Filler. The application process of the CFRP divided into two parts: Painting the surface with Skiadur330 epoxy resin, and then apply the longitudinal layer of the unidirectional CFRP Skiawrap230C. This longitudinal layer was applied to counteract the concrete transverse cracks at plastic hinge zone. This layer has L-shaped; 20cm glued to the column and 10 cm glued to the footing. For confining purposes, another layer of the Skiadur330 epoxy resin was painted and then transverse layer of the Skiawrap230C was wrapped. The wrapped layer width is 30cm which is equal to the length of the plastic hinge. Wrapping length is 150cm which is equal to the column perimeter in addition to 10 cm overlap required by the Egyptian Code of Practice for FRP. Finally, extra layer of Skiadur330 epoxy resin was painted to insure full saturation of the CFRP with epoxy. Fig. 4 illustrates the repair process. It is worthy to mention that the specimen S1, which did not contain steel fiber consumes double amount Skiadur31CF and Sikadure501 Filler compared to any other of the repaired specimens. This was due to big amount of damaged concrete as illustrated in Fig 3.

(a) (b)

Fig. 2: Preparing of specimens, a) Removing loose concrete, b) Removing dust

(a) (b) (c) (d)

Fig. 3: Specimens after removing loose concrete a) S1, b) S2, c) S6, d) S7

(a) (b) (c)

(d) (e) (f)

Fig. 4: Repair process, a) Application of Sikadure31CF, b) Rounded corners, c) Application of Skiadur330 d) Application of longitudinal Skiawrap230C e) Wrapping of transverse Skiawrap230C, f) Adding extra layer of Skiadur330

2.3 Test Setup

To study the efficiency of using CFRP as repair material for SFRC in bridge columns witch resisting earthquakes, the hysteretic behavior was examined through Quasi-static tests of repeated lateral load in the presence of constant axial compressive load. These tests were performed in the reinforced concrete laboratory of the housing and building research center (HBRC) at Giza, Egypt. Fig. 5 illustrates the test setup. Two lateral

LVDTs (Linear Voltage Displacement Transducers) located at 0.90m and 1.80 from footing top were attached to the specimen.

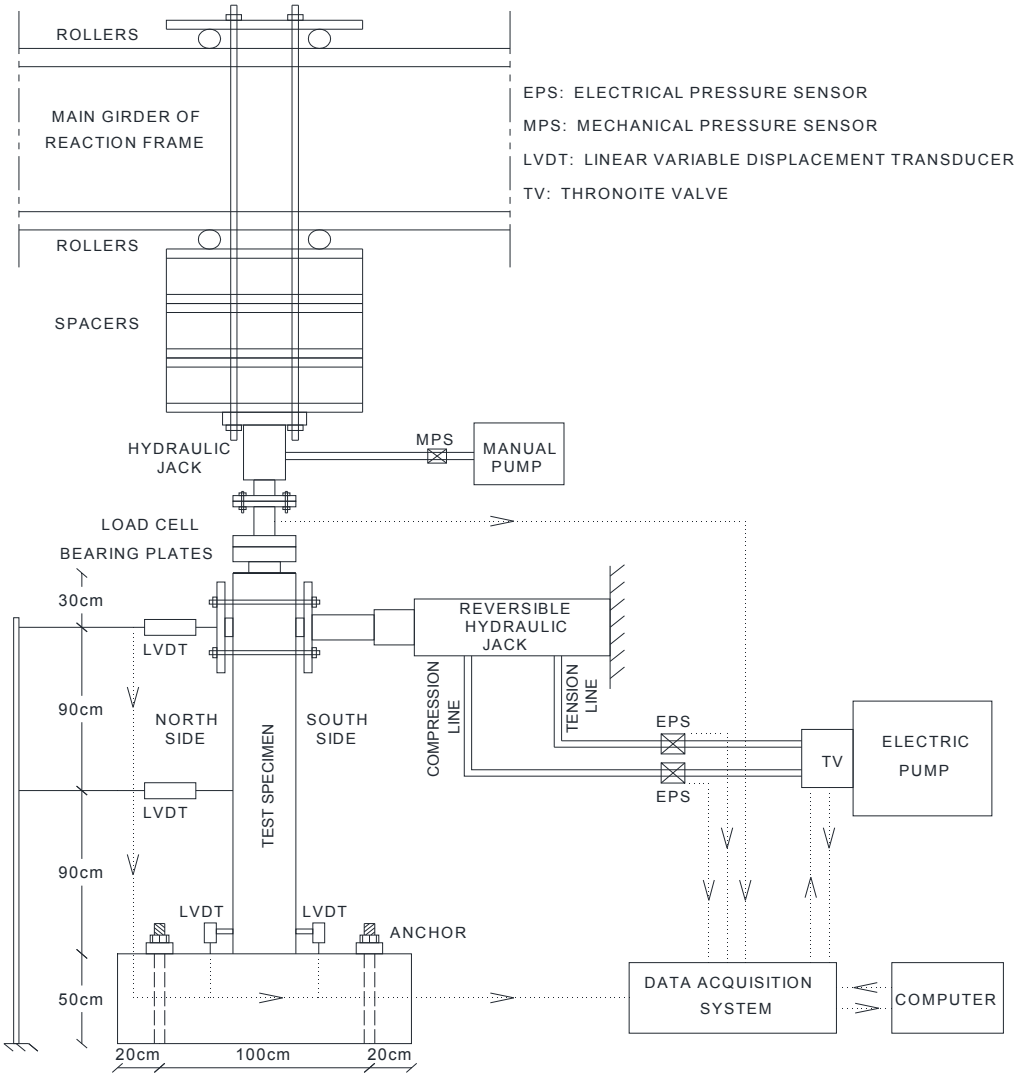

Fig. 5: Schematic of test setup [1]

2.3 Testing Procedure

An axial compression force of 588 KN was applied through a hydraulic jack on the top of column, then the lateral jack was attached and its screws were fastened. Then, the screws of the lateral LVDTs were fastened and all wires of the LVDTs were connected to the data acquisition system. Next step is to reset all readings in the data acquisition system, and then start to apply the displacement protocol as illustrated in Fig. 6. Displacement scenario was selected based on ATC-24 protocol [19]. The system automatically saves the measured displacement, the measured lateral load and all recorded data from the LVDTs, and axial load cell.

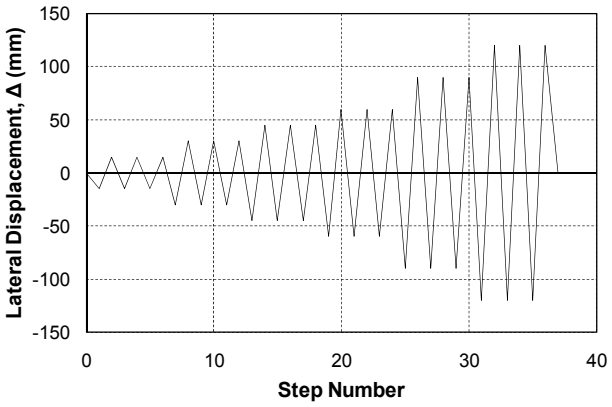

Fig. 6: Loading scenario of tests [1]

3. EXPERIMENTAL RESULTS, ANALYSIS AND DISCUSSION

3.1 Modes of Failure

All specimens were selected such that the shear span to depth ratio equal to 6, all specimens were failed in bending by developing plastic hinge at column bottom[1]. The Longitudinal layer of CFRP resisted the development of transverse cracks at plastic hinge zone. While the transverse layer CFRP provided well confining to concrete, therefore the plastic hinge zone kept in a good state until the test end. A separation crack between column and footing was developed to absorb the column rotation. No complete deboning was occurred until test end, but progressive deboning between the horizontal part of the longitudinal CFRP layer and top of footing. The transverse CFRP layer remained in its original state up to test end. Fig. 7 illustrates the mode of failure for all repaired specimens.

(a) (b) (c) (d)

Fig. 7: Mode of failure for repaired specimens, a) S1R, b) S2R , c) S6R, d) S7R

3.2 Load–Displacement Relationships and Strength Evaluation

The load-displacement hysteresis loops for both original and repaired specimens are illustrated in Fig. 8. It can be noticed that the repaired specimen behaved well and the hysteretic behavior was well recovered. The ultimate load was approximately recovered. The experimentally determined yield displacement was approximately doubled except for S7 it was about one and one half the original value. It is worthy to mention that for the first few cycles, the initial strength was not recovered due to previous yielding of the longitudinal reinforcement bars. Table 1 provides numerical comparison between some of the hysteretic indicators such as the ultimate load, the lateral displacement corresponding ultimate load, the failure displacement, and the yield displacement.

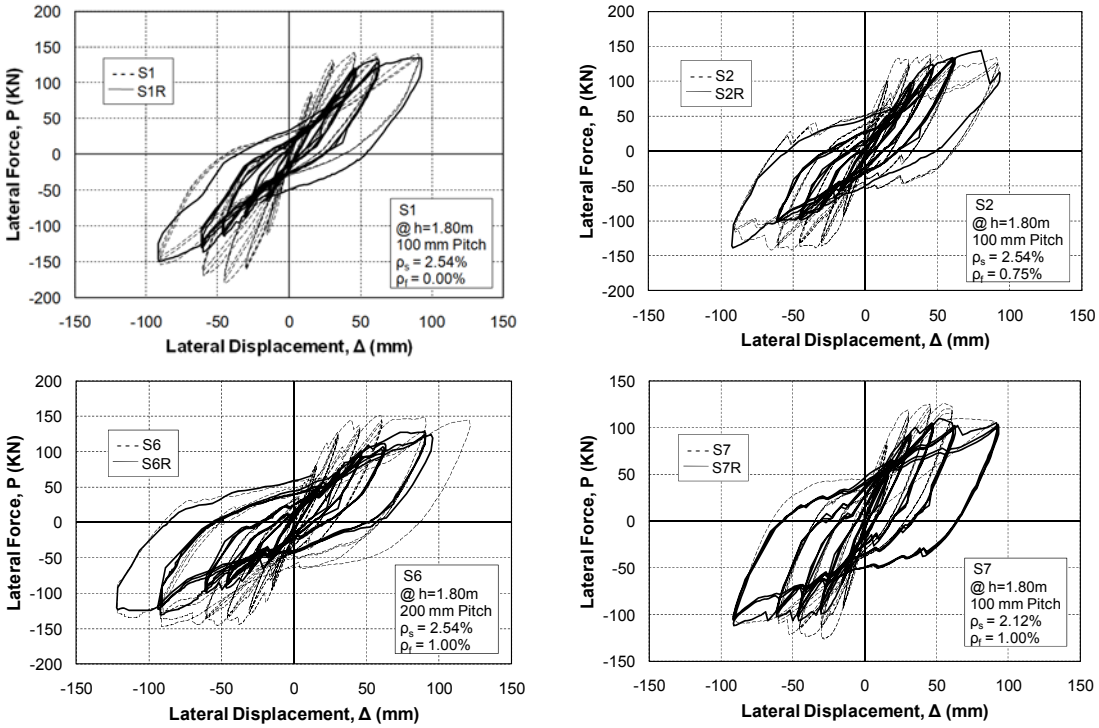

Fig. 8: Hysteresis loops for original and repaired specimens

Table 1: The experimental results of original and repaired specimens

SPECIMEN	P_1 (first cycle load at 7.5 mm displacement) (KN)	P_u (Ultimate load) (KN)	Δ_u (displacement at Pu (mm)	Δ_f (displacement at failure) (mm)	Δ_y (Yeild displacement) (mm)
S1	52.70	164.65	75.78	>91.03	25.34
S1R	40.96	149.24	91.17	>92.70	50.10
S2	58.35	141.88	65.44	>122.28	21.03
S2R	32.28	144.30	80.18	>93.24	48.08
S6	53.24	151.11	60.031	>121.89	27.67
S6R	33.29	130.52	91.96	>95.76	57.13
S7	58.49	126.11	28.51	>90.44	20.08
S7R	36.36	110.12	52.02	>93.18	31.26

3.3 Yield, Failure Displacement, Displacement Ductility Factor and Accumulated Displacement Ductility

The yield displacement for an equivalent elastic-plastic system with reduced cracked stiffness was calculated from the lateral load-displacement curve as the corresponding displacement of intersection of the secant stiffness (at either the first yield or at a load value of 75% of the ultimate lateral load whichever is less) and a tangent stiffness at the ultimate load. The first yield could not be accurately determined during the test program; hence the evaluation of yield displacement is based on the value of 75% of ultimate lateral load as shown in Fig. 9.

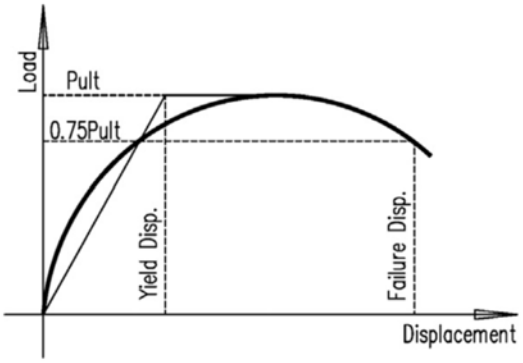

Fig. 9: Determination of yield and failure displacement.

The displacement ductility is defined as the ratio between the maximum displacement at cyclic number *i*, Δ*i*, and the yield displacement Δy.

$$\textbf{Displacement ductility} = \Delta i / \Delta y \quad (1)$$

Also, the displacement ductility factor is defined as the ratio between the displacement at failure, Δ*f*, and the yield displacement Δ*y*.

$$\textbf{Displacement ductility factor} = \Delta f / \Delta y \quad (2)$$

The accumulated displacement ductility is defined as the sum of the displacement ductility up to the defined failure load.

$$\textbf{Accumulated displacement ductility} = \Sigma (\Delta i / \Delta y) \quad (3)$$

where Δ*i* is the maximum displacement at cycle number *i*.

Table 2 provides numerical comparison of the displacement ductility factors and the accumulated displacement ductility for the original and repaired specimens. It can be noticed that the displacement ductility and ductility factor were highly affected by the increase of the experimentally determined yield displacement. The Accumulated Ductility up to 5% top drift ratio dropped to about half its original value except for S7 it dropped to about two third its original value.

Table 2: Displacement ductility factor

SPECIMEN	Displacement ductility factor	Accumulated Ductility up to 5% top drift ratio
S1	>3.59	28.75

S1R	>1.82	14.77
S2	>5.81	34.51
S2R	>1.94	14.69
S6	>4.41	26.33
S6R	>1.68	12.94
S7	>4.50	36.08
S7R	>2.98	23.49

3.4 Energy Dissipation Characteristics

The capability of a structure to withstand an earthquake depends on its ability to dissipate the energy input from ground motion. Despite the fact that energy input during a earthquake is difficult to estimate, a satisfactory design should ensure a larger energy dissipation capability of the structure than the demand. Fig. 10 illustrates the variation of the cumulative dissipated energy with the lateral displacement for original and repaired specimens. The dissipated energy was computed for each cycle as the area enclosed by the lateral load–displacement hysteresis loop for the cycle. The area was computed using Eq. (4).

$$E_i = [\,(P_{i+1} + P_i) * (\Delta_{i+1} - \Delta_i) / 2] \quad (4)$$

Where E_i energy dissipated per cycle, Pi and $Pi+1$ are the lateral loads at intervals number i, and $i+1$, Δ_i and Δ_{i+1} are the lateral displacement at intervals number i, and $i+1$.

A non dimensional energy index is used to evaluate the energy dissipated by different test specimens. In the current study, the normalized energy index (I_{EN}), proposed by Ehsani and Wight [20] was used as a reliable and comprehensive measure of dissipated energy. It has the advantage of including the effect of actual displacement, stiffness and energy for each cycle. Consequently, this index is sensitive in evaluating any variations in the seismic performance of beam-column joints. The normalized energy index, IEN, is expressed as follows:

$$I_{EN} = \frac{1}{P_y \Delta_y} \sum_{i=1}^{m} E_i \left(\frac{K_i}{K_y} \right) \left(\frac{\Delta_i}{\Delta_y} \right)^2 \quad (5)$$

Where E_i is the energy dissipated during *ith* cycle of loading, Δ_y is the yield displacement of the specimen, P_y is the yield load, K_y is the stiffness corresponding to the yield displacement and, Δ_i is the peak displacement of the *ith* cycle and K_i is the corresponding stiffness. The specimen having a normalized energy dissipation index of 60 or higher possesses sufficient ductility to satisfy the requirements of Committee 352 recommendations [21]. Table 3 and table 4 summarize these results. It can be noticed that the presence of the steel fibers increased the recovered absorbed energy. The energy index was decreased for all repaired specimens due to the increase of the experimentally determined yield displacement.

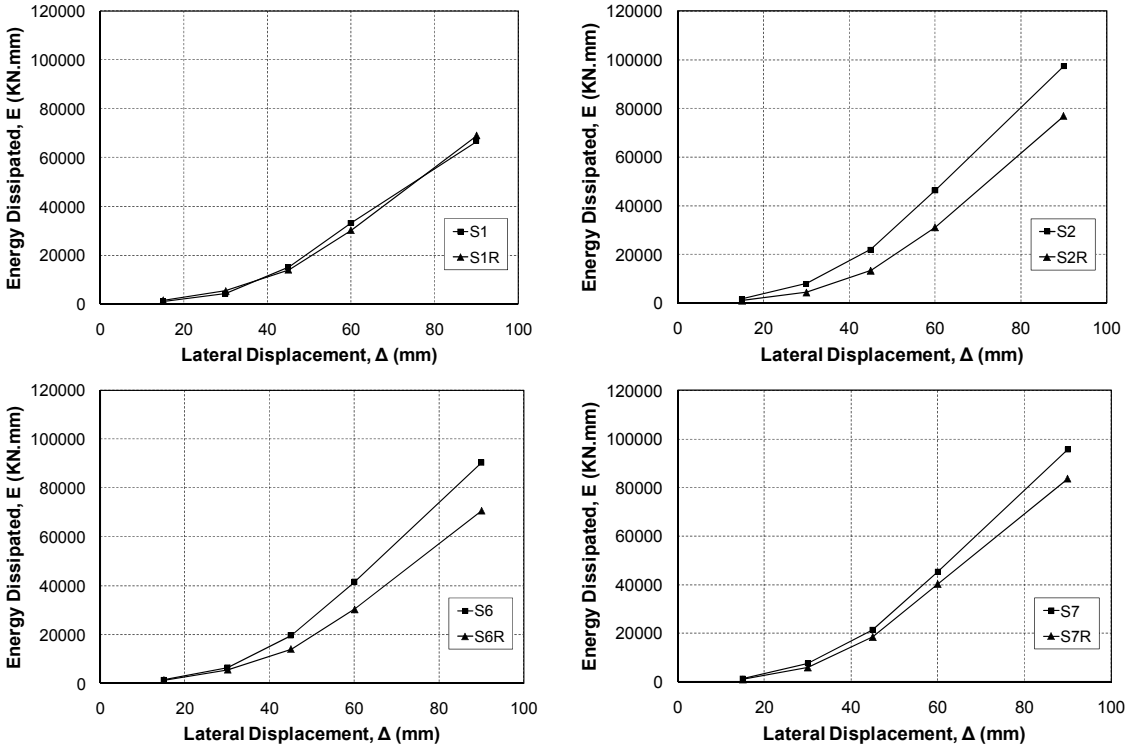

Fig. 10: Energy dissipation for original and repaired specimens

Table 3: Accumulated energy at different lateral displacement levels

SPECIMEN	Accumulated energy, E (KN.mm)				
	15mm	30mm	45mm	60mm	90mm
S1	1118.76	4318.34	15139.80	33251.48	66742.51
S1R	1591.63	5488.43	14067.83	30233.75	69091.29
S2	1616.15	7857.71	21934.88	46274.30	97235.53
S2R	961.97	4286.86	13242.67	31044.51	76817.11
S6	1357.03	6475.69	19590.90	41475.37	90354.81
S6R	1283.69	5564.51	13997.14	30357.30	70590.30
S7	1303.44	7537.15	21415.59	45249.34	95568.81
S7R	1027.66	5972.13	18466.07	40320.03	83635.91

Table 4: Total accumulated energy and the energy index of the specimens

SPECIMEN	Total accumulated energy up to test end (KN. mm)	Total accumulated energy up to 5% top drift ratio (KN. mm)	IEN (up to 5% top drift ratio)
S1	66742.51	66742.51	54.41
S1R	69091.30	69091.30	15.15
S2	126186.90	97235.53	129.97
S2R	76817.11	76817.11	20.07
S6	117659.40	90354.81	68.19
S6R	70590.30	70590.30	14.38
S7	95568.82	95568.82	128.32
S7R	83635.91	83635.91	78.44

3.5 Stiffness Analysis

The cracked stiffness of each of the specimens was calculated for every loading cycle. The cracked stiffness was computed as follows:

$$K_i = P_i / \Delta_i \quad (6)$$

where: P_i is the maximum load at cycle i , and Δ_i is the maximum displacement at cycle i. The cracked stiffness versus the lateral displacement to represent the stiffness degradation due to cyclic loading of the tested eight specimens is illustrated in Fig. 11 and table 5. It can be concluded that the stiffness was not completely recovered due to the previous yielding of the longitudinal reinforcement bars, but the gap decreased with the increase of the deformation level and with the increase of the steel fiber content.

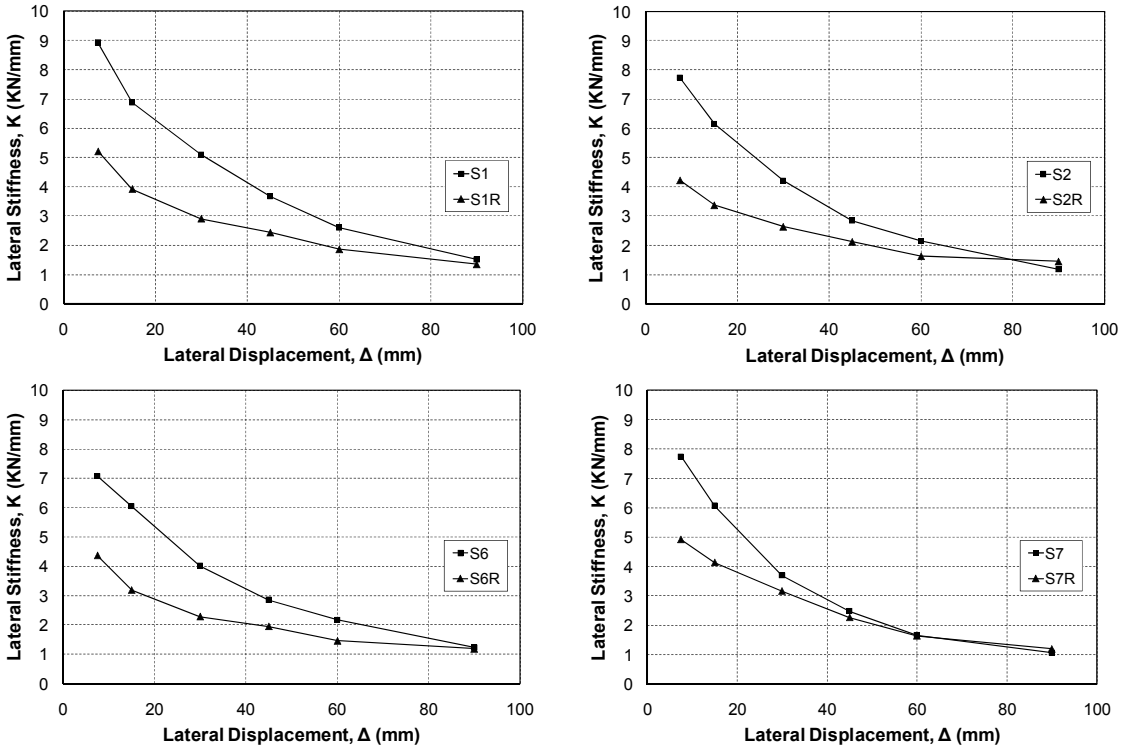

Fig. 11: Stiffness degradation of original and repaired specimens**.**

Table 5: Lateral Stiffness at different lateral displacement levels

SPECIMEN	Lateral Stiffness, K (KN/mm)					
	7.5mm	15mm	30mm	45mm	60mm	90mm
S1	8.92	6.87	5.09	3.66	2.60	1.50
S1R	5.21	3.91	2.90	2.43	1.86	1.35
S2	7.73	6.15	4.21	2.85	2.15	1.18
S2R	4.23	3.38	2.64	2.13	1.64	1.46
S6	7.07	6.04	4.01	2.85	2.17	1.23
S6R	4.36	3.18	2.28	1.95	1.46	1.19
S7	7.74	6.07	3.69	2.48	1.66	1.06
S7R	4.92	4.14	3.16	2.26	1.64	1.20

4. CONCLUSIONS

The hysteretic behavior of SFRC bridge column specimens was recovered through repairing the damaged specimens using CFPR. The repair process consisted of three main stages and was kept the same for all specimens. Repair stages started with replacing the lose concrete by epoxy mortar, and then added one longitudinal CFRP layer to counteract the formation of transverse cracks, and finally one wrapping transverse CFRP layer for confining purposes.

The presence of the steel fibers facilitates the repair process and reduces its cost by retaining the integrity of the plastic hinge zone, so that minimize the amount of the used epoxy mortar. The ultimate load was approximately recovered. The experimentally determined yield displacement was approximately doubled except for S7 it was about one and one half the original value. The displacement ductility and ductility factors were highly affected by the increase of the experimentally determined yield displacement. The Accumulated Ductility up to 5% top drift ratio dropped to about half its original value except for S7 it dropped to about two third its original value. The recovered absorbed energy increased with the increase of the steel fiber content. The energy index was decreased for all repaired specimens due to the increase of the experimentally determined yield displacement. The stiffness was not completely recovered due to the previous yielding of the longitudinal reinforcement bars, but the gap decreased with the increase of the deformation level and with the increase of the steel fiber content.

The mode of failure for all specimens is a major separation crack between column and footing. Well confined plastic hinge region led to develop this crack to absorb the column rotation. No complete deboning was occurred until test end, but progressive deboning between the horizontal part of the longitudinal CFRP layer and top of footing. The transverse CFRP layer remained in its original state up to test end.

REFERENCES

[1] Naguib A. M., El-Esnawy N. A., Saleh A. M., and Atteya W. A., “Hysteretic Behavior of Steel Fiber Reinforced Concrete Bridge Columns”, Civil Engineering Research Magazine, Faculty of Engineering, Al-Azhar University; 39(1):252-273, 2017.

[2] American Concrete Institute (ACI) Committee 544, “Report on Fiber Reinforced Concrete”, ACI544.1R-96: (Reapproved 2009), Farmington Hills, USA, 1996.

[3] American Concrete Institute (ACI) Committee 544, “Measurement of Properties of Fiber Reinforced Concrete”, ACI 544.2R-89: (Reapproved 2009), Farmington Hills, USA, 1989.

[4] American Concrete Institute (ACI) Committee 544, “Guide for Specifying, Proportioning, and Production of Fiber-Reinforced Concrete”, ACI 544.3R-08, Farmington Hills, USA, 2008.

[5] American Concrete Institute (ACI) Committee 544, “Design Considerations for Steel Fiber Reinforced Concrete, ACI 544.4R-88 :(Reapproved 2009), Farmington Hills, USA, 1988.

[6] American Concrete Institute (ACI) Committee 544, “Report on the Physical Properties and Durability of Fiber-Reinforced Concrete”, ACI 544.5R-10, Farmington Hills, USA, 2010.

[7] European Committee for Standardization (CEN/TC 104), "Fibres for concrete", EN 14889-1:2006, United Kingdom, 2006.
[8] American Society for Testing and Materials, (ASTM) Committee A01.05, "Standard Specification for Steel Fibers for Fiber-Reinforced Concrete", ASTM A820 / A820M - 11, ASTM International, West Conshohocken, PA, USA, 2011.
[9] Applied Technology Council (ATC), "Seismic Design Criteria for Bridges and Other Highway Structures: Current and Future", ATC-18, Redwood City, CA, 1997.
[10] Hussein Y., "Seismic Behavior of Strengthened Reinforced Concrete Columns", PhD Thesis, Faculty of Engineering, Cairo University, Giza, Egypt, 1999.
[11] Mohamedien M., Hosny A., and Abdelrahman A., "Use of FRP in Egypt, Research Overview and Applications", Procedia Engineering; 54, 2 – 21, 2013.
[12] Seliem H., "Seismic Retrofit of Reinforced Concrete Columns Using Fiber-Reinforced Polymer Jackets", MSc. Thesis, Faculty of Engineering, Cairo University, Giza, Egypt, 2002.
[13] Ahmed A. F., "Strengthening of Rectangular Reinforced Concrete Columns Using Fiber Glass Reinforced Polymers", MSc. Thesis, Faculty of Engineering, Cairo University, Giza, Egypt, 2009.
[14] Kamel T. M., "Durability and Bond Characterestics of Concrete Elements Reinforced With Various FRP Strengthening Techniques", PhD Thesis, Faculty of Engineering, Ain Shams University, Cairo, Egypt, 2008.
[15] He R., Sneed L. H., and Belarbi A., "Rapid repair of Severely Damaged RC Columns with Different Damage Conditions – An Experimental Study", International Journal of Concrete Structures and Materials; 7(1), 35-50, 2013.
[16] Egyptian Code of Practice (ECP) Committee 208, "Egyptian Code of Practice for the Use of Fiber Reinforced Polymer (FRP) in the Construction Fields", Housing and Building National Research Center, Giza, Egypt, 2005.
[17] ACI Committee 440, "Guide for the design and construction of externally bonded FRP systems for strengthening concrete structures", ACI 440.R-08, Farmington Hills, MI: American Concrete Institute, 2008.
[18] Contractor Business Unit at Sika Egypt, "Products Catalog and Technical Data Sheets", sixth edition, Elobour city, Egypt, 2010 (http://www.sika.com.eg).
[19] Applied Technology Council (ATC), "Guidelines for Cyclic Seismic Testing of Components of Steel Structures", ATC-24, Applied Technology Council, Redwood City, CA, 1992.
[20] M.R. Ehssani, and J.K. Wight, "Confinement steel requirements for connection ductile frames", J. Struct. Eng. 116; 450–465, 1990.
[21] ACI-ASCE Committee 352, "Recommendations for Design of Beam-Column Connections in Monolithic Reinforced Concrete Structures", American Concrete Institute, 2002.